



Tensor Métrico Cuántico en el modelo de Dicke

Instituto de
Ciencias
Nucleares
UNAM



Jorge Chávez Carlos, Daniel Gutiérrez-Ruiz, Diego González, J. David Vergara, Jorge G. Hirsch

ICN, UNAM

Caos y localización en sistemas cuánticos de muchos cuerpos

24-26 Enero 2022

Outline

- Antecedentes
- Conceptos
- Tensor geométrico cuántico en el modelo LMG
- Tensor métrico cuántico en el modelo de Dicke
- Conclusiones

Information-Theoretic Differential Geometry of Quantum Phase Transitions

Paolo Zanardi, Paolo Giorda, and Marco Cozzini
Phys. Rev. Lett. **99**, 100603 – Published 7 September 2007




[Article](#)[References](#)[Citing Articles \(295\)](#)[PDF](#)[HTML](#)[Export Citation](#)

ABSTRACT

The manifold of coupling constants parametrizing a quantum Hamiltonian is equipped with a natural Riemannian metric with an operational distinguishability content. We argue that the singularities of this metric are in correspondence with the quantum phase transitions featured by the corresponding system. This approach provides a universal conceptual framework to study quantum critical phenomena which is differential geometric and information theoretic at the same time.

PAPER

Phase space formulation of the Abelian and non-Abelian quantum geometric tensor

Diego Gonzalez^{3,1,2} , Daniel Gutiérrez-Ruiz¹  and J David Vergara¹ 

Published 23 November 2020 • © 2020 IOP Publishing Ltd

[Journal of Physics A: Mathematical and Theoretical, Volume 53, Number 50](#)

Citation Diego Gonzalez et al 2020 *J. Phys. A: Math. Theor.* **53** 505305

[+ Article information](#)

Abstract

The geometry of the parameter space is encoded by the quantum geometric tensor, which captures fundamental information about quantum states and contains both the quantum metric tensor and the curvature of the Berry connection. We present a formulation of the Berry connection and the quantum geometric tensor in the framework of the phase space or Wigner function formalism. This formulation is obtained through the direct application of the Weyl correspondence to the geometric structure under consideration. In particular, we show that the quantum metric tensor can be computed using only the Wigner functions, which opens an alternative way to experimentally measure the components of this tensor. We also address the non-Abelian generalization and obtain the phase space formulation of the Wilczek–Zee connection and the non-Abelian quantum geometric tensor. In this case, the non-Abelian quantum metric tensor involves only the non-diagonal Wigner functions. Then, we verify our approach with examples and apply it to a system of N coupled harmonic oscillators, showing that the associated Berry connection vanishes and obtaining the analytic expression for the quantum metric tensor. Our results indicate that the developed approach is well adapted to study the parameter space associated with quantum many-body systems.

¹ P. Zanardi, P. Giorda, and M. Cozzini, Phys. Rev. Lett. **99**, 100603 (2007).

² D. González, D. Gutiérrez-Ruiz, and J. D. Vergara, J. Phys. A: Math. Theor. **53**, 505305 (2020).

Rapid Communication

Extracting the quantum metric tensor through periodic driving

Tomoki Ozawa and Nathan Goldman

Phys. Rev. B **97**, 201117(R) – Published 31 May 2018
[Article](#)
[References](#)
[Citing Articles \(36\)](#)
[Supplemental Material](#)
[PDF](#)
[HTML](#)
[Export Citation](#)


ABSTRACT

We propose a generic protocol to experimentally measure the quantum metric tensor, a fundamental geometric property of quantum states. Our method is based on the observation that the excitation rate of a quantum state directly relates to components of the quantum metric upon applying a proper time-periodic modulation. We discuss the applicability of this scheme to generic two-level systems, where the Hamiltonian's parameters can be externally tuned, and also to the context of Bloch bands associated with lattice systems. As an illustration, we extract the quantum metric of the multiband Hofstadter model. Moreover, we demonstrate how this method can be used to directly probe the spread functional, a quantity which sets the lower bound on the spread of Wannier functions and signals phase transitions. Our proposal offers a universal probe for quantum geometry, which could be readily applied in a wide range of physical settings, ranging from superconducting quantum circuits to ultracold atomic gases.

Experimental Measurement of the Quantum Metric Tensor and Related Topological Phase Transition with a Superconducting Qubit

Xinsheng Tan, Dan-Wei Zhang, Zhen Yang, Ji Chu, Yan-Qing Zhu, Danyu Li, Xiaopei Yang, Shuqing Song, Zhikun Han, Zhiyuan Li, Yuqian Dong, Hai-Feng Yu, Hui Yan, Shi-Liang Zhu, and Yang Yu

Phys. Rev. Lett. **122**, 210401 – Published 29 May 2019; Erratum [Phys. Rev. Lett.](#) **123**, 159902 (2019)
[Article](#)
[References](#)
[Citing Articles \(35\)](#)
[Supplemental Material](#)
[PDF](#)
[HTML](#)
[Export Citation](#)


ABSTRACT

A Berry curvature is an imaginary component of the quantum geometric tensor (QGT) and is well studied in many branches of modern physics; however, the quantum metric as a real component of the QGT is less explored. Here, by using tunable superconducting circuits, we experimentally demonstrate two methods to directly measure the quantum metric tensor for characterizing the geometry and topology of underlying quantum states in parameter space. The first method is to probe the transition probability after a sudden quench, and the second one is to detect the excitation rate under weak periodic driving. Furthermore, based on quantum metric and Berry-curvature measurements, we explore a topological phase transition in a simulated time-reversal-symmetric system. The work opens up a unique approach to explore the topology of quantum states with the QGT.

³ T. Ozawa and N. Goldman, Phys. Rev. B **97**, 201117(R) (2018).

⁴ X. Tan, D.-W. Zhang, Z. Yang, J. Chu, Y.-Q. Zhu, D. Li, X. Yang, S. Song, Z. Han, Z. Li, Y. Dong, H.-F. Yu, H. Yan, S.-L. Zhu, and Y. Yu, Phys. Rev. Lett. **122**, 210401 (2019).

Tensor Geométrico Cuántico (QGT)

- Tensor Geométrico Cuántico (Quantum Geometric Tensor - QGT)⁴
- Estudio de Transiciones de Fase usando Geometría Cuántica⁵
- Ayuda a medir **distancia** en el espacio de parámetros $X = \{X^i\}$, $i = 1, \dots, m$ entre dos estados cuánticos con un desplazamiento infinitesimal de parámetros.

$$|n_X\rangle$$

$$|n_{X+\delta X}\rangle$$

$$Q_{ij}^{(n)} := \langle \partial_i n | \partial_j n \rangle - \langle \partial_i n | n \rangle \langle n | \partial_j n \rangle,$$

$$\hat{H}|n\rangle = E_n|n\rangle \quad y \quad \partial_i = \partial/\partial X_i$$

- QGT similar a la **fidelidad**⁶

⁴ J. P. Provost and G. Vallee, Commun. Math. Phys. **76**, 289 (1980).

⁵ A. Carollo, D. Valenti, and B. Spagnolo, Phys. Rep. **838**, 1 (2020).

⁶ W. K. Wootters, Phys. Rev. D **23**, 357 (1981).

Tensor Métrico Cuántico (QMT)

- Partimos de QGT⁷

$$Q_{ij}^{(n)} = \sum_{m \neq n} \frac{\langle n | \partial_i \hat{H} | m \rangle \langle m | \partial_j \hat{H} | n \rangle}{(E_m - E_n)^2}$$

- Curvatura de Berry: Im(QGT)
- Tensor Métrico Cuántico (QMT): Re(QGT)

$$g_{ij}^{(n)} = \text{Re } Q_{ij}^{(n)}$$

⁷S.-J. Gu, Int. J. Mod. Phys. B **24**, 4371 (2010).

Escalar de curvatura R (Escalar de Ricci)

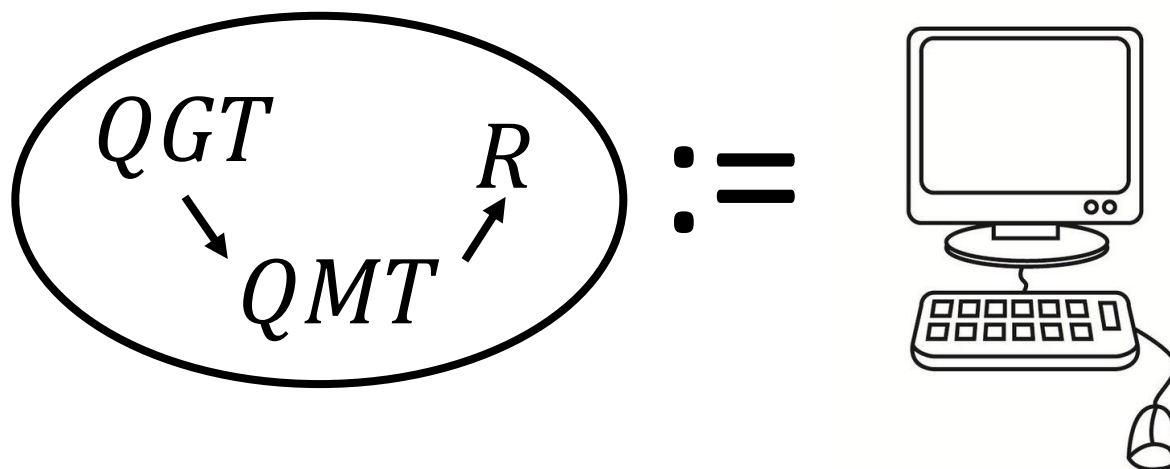
- Cantidad invariante ante el espacio de parámetros usados en su cálculo.
- Para un espacio de parámetros plano: $X = \{X^1, X^2\}$ se puede usar:

$$R = \frac{1}{\sqrt{|g|}} (\mathcal{A} + \mathcal{B})$$

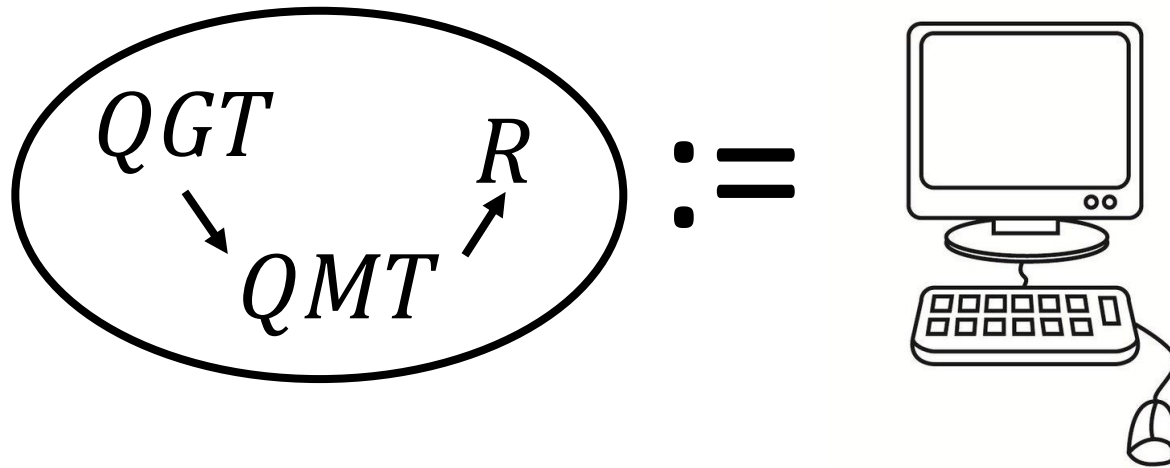
$$\mathcal{A} := \partial_1 \left(\frac{g_{12}}{g_{11}\sqrt{|g|}} \partial_2 g_{11} - \frac{1}{\sqrt{|g|}} \partial_1 g_{22} \right) \quad \mathcal{B} := \partial_2 \left(\frac{2}{\sqrt{|g|}} \partial_1 g_{12} - \frac{1}{\sqrt{|g|}} \partial_2 g_{11} - \frac{g_{12}}{g_{11}\sqrt{|g|}} \partial_1 g_{11} \right)$$

Donde $g = \det[g_{ij}]$

Manos a la obra

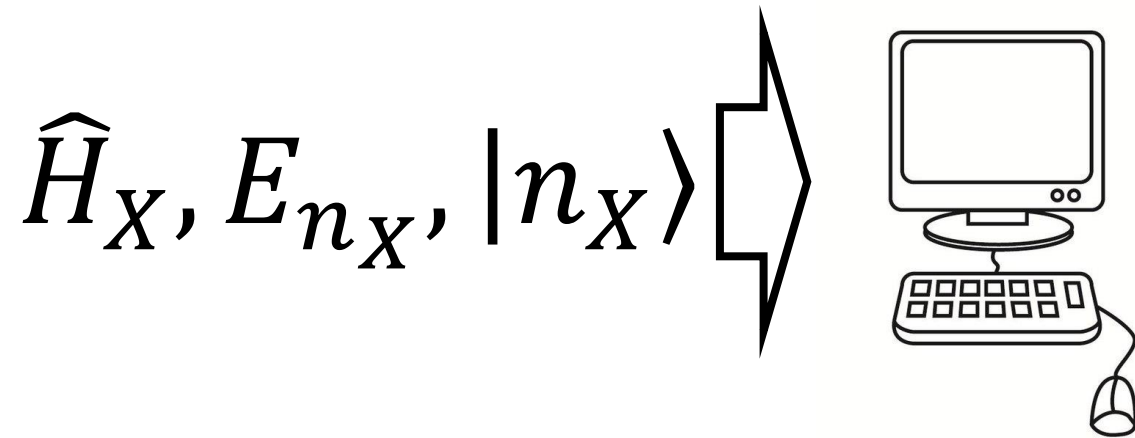
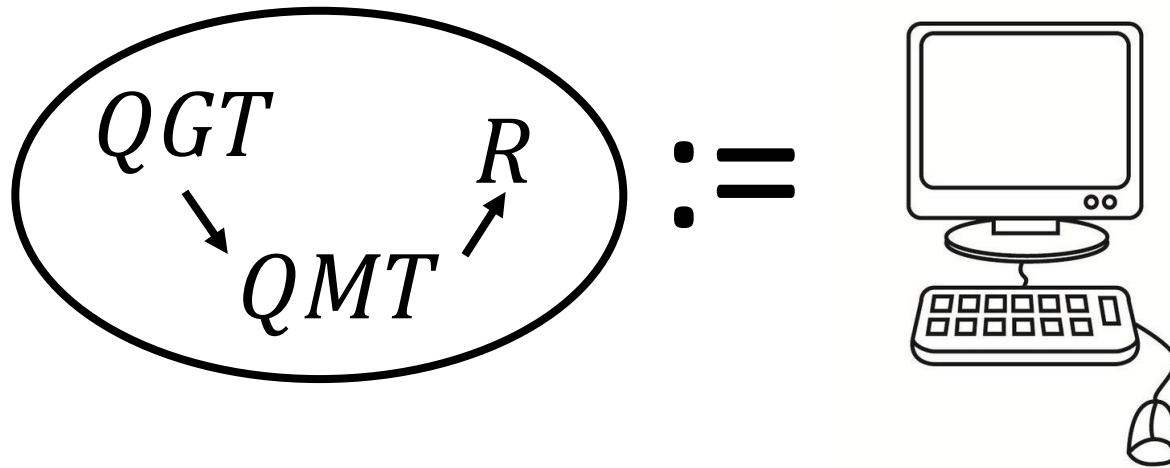


Manos a la obra

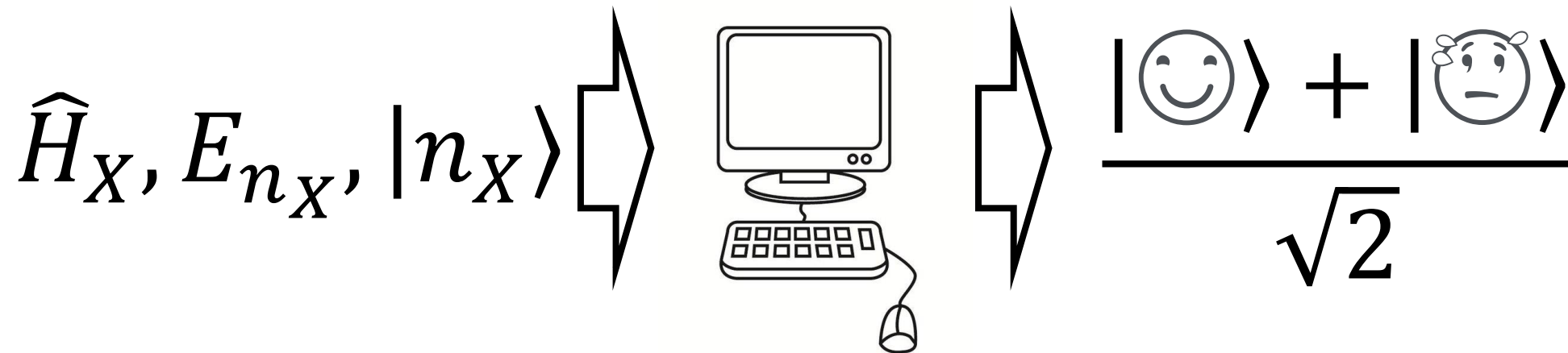
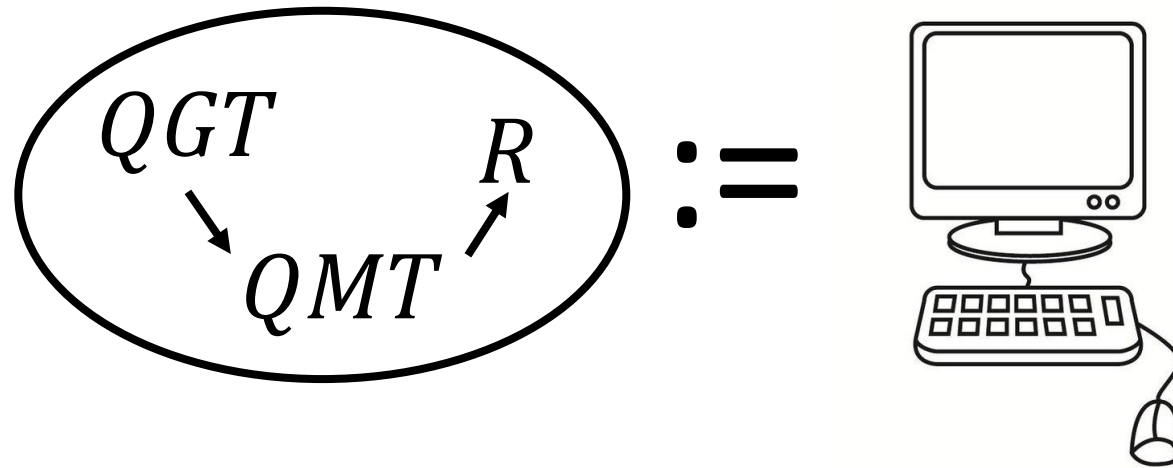


$$\hat{H}_X, E_{n_X}, |n_X\rangle$$

Manos a la obra








Manos a la obra



QGT en el modelo LMG

PHYSICAL REVIEW B **103**, 174104 (2021)

Quantum geometric tensor and quantum phase transitions in the Lipkin-Meshkov-Glick model

Daniel Gutiérrez-Ruiz ^{1,*} Diego Gonzalez ^{1,2,†} Jorge Chávez-Carlos ^{3,‡} Jorge G. Hirsch ^{1,§} and J. David Vergara ^{1,||}

¹*Instituto de Ciencias Nucleares, Universidad Nacional Autónoma de México, Apartado Postal 70-543, Ciudad de México 04510, México*

²*Departamento de Física, Cinvestav, Avenida Instituto Politécnico Nacional 2508, San Pedro Zacatenco, 07360 Gustavo A. Madero, Ciudad de México, México*

³*Instituto de Ciencias Físicas, Universidad Nacional Autónoma de México, Cuernavaca, Morelos 62210, México*



Received 26 January 2021; revised 15 April 2021; accepted 27 April 2021; published 10 May 2021)

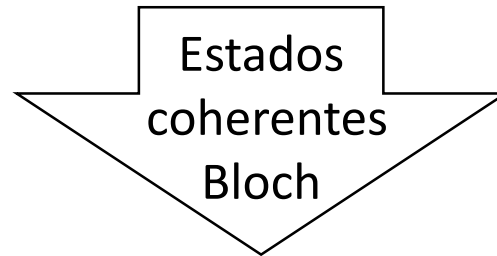


We study the quantum metric tensor and its scalar curvature for a particular version of the Lipkin-Meshkov-Glick model. We build the classical Hamiltonian using Bloch coherent states and find its stationary points. They exhibit the presence of a ground-state quantum phase transition where a bifurcation occurs, showing a change in stability associated with an excited-state quantum phase transition. Symmetrically, for a sign change in one Hamiltonian parameter, the same phenomenon is observed in the highest-energy state. Employing the Holstein-Primakoff approximation, we derive analytic expressions for the quantum metric tensor and compute the scalar and Berry curvatures. We contrast the analytic results with their finite-size counterparts obtained through exact numerical diagonalization and find excellent agreement between them for large sizes of the system in a wide region of the parameter space except in points near the phase transition where the Holstein-Primakoff approximation ceases to be valid.

DOI: [10.1103/PhysRevB.103.174104](https://doi.org/10.1103/PhysRevB.103.174104)

LMG

$$\hat{H}_{\text{LMG}} = \Omega \hat{J}_z + \Omega_x \hat{J}_x + \frac{\xi_y}{j} \hat{J}_y^2$$



$$H_{\text{LMG}}(Q, P) = \frac{\Omega}{2} (Q^2 + P^2) - \Omega + \Omega_x Q \sqrt{1 - \frac{Q^2 + P^2}{4}} + \xi_y P^2 \left(1 - \frac{Q^2 + P^2}{4}\right).$$

Con $\Omega = 1$, espacio de parámetros $X = \{\Omega_x, \xi_y\}$

$$\Omega_{xc} = \sqrt{4\xi_y^2 - 1}$$

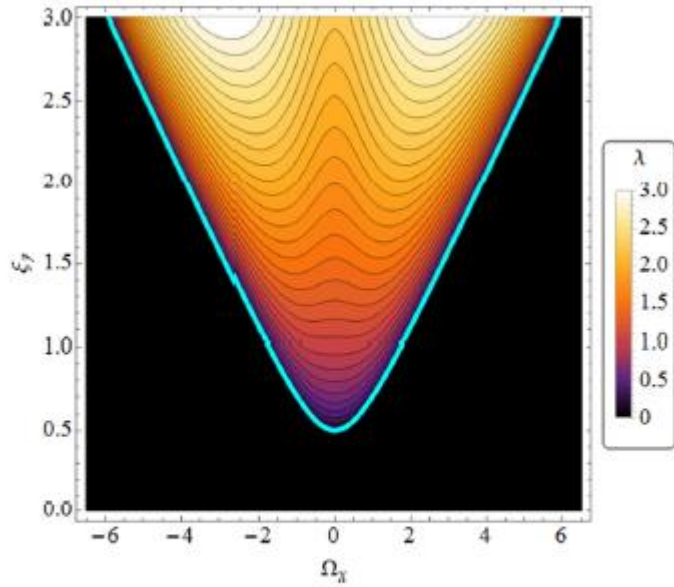


FIG. 4. Lyapunov exponent for the stationary point x_1 as a function of the coupling parameters Ω_x and $\xi_y > 0$. The black zone indicates a null Lyapunov exponent.

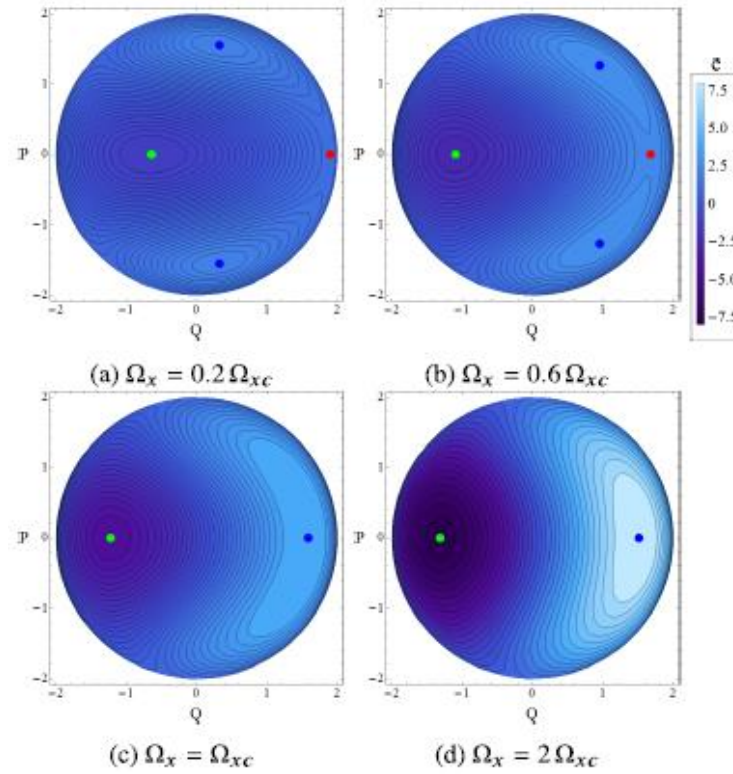


FIG. 5. Energy surfaces for different values of the parameters Ω with $\Omega_{xc} = \sqrt{4\xi_y^2 - 1}$ with $\xi_y = 2$. Green points are stable center points x_2 , the blue ones are unstable center points: x_4 and x'_4 in (a) and (b), and in (c) and (d), the red point is the stationary point with positive Lyapunov exponent x_1 , only present in (a) and (b).

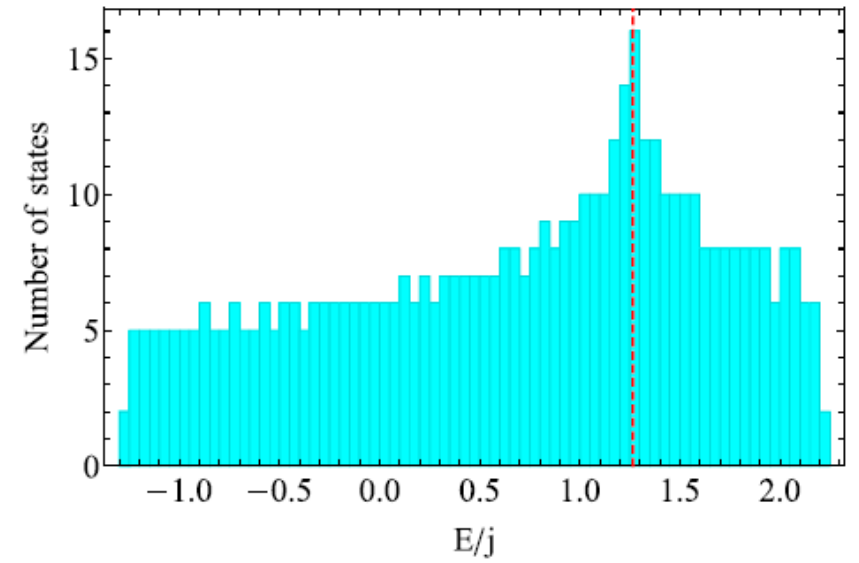


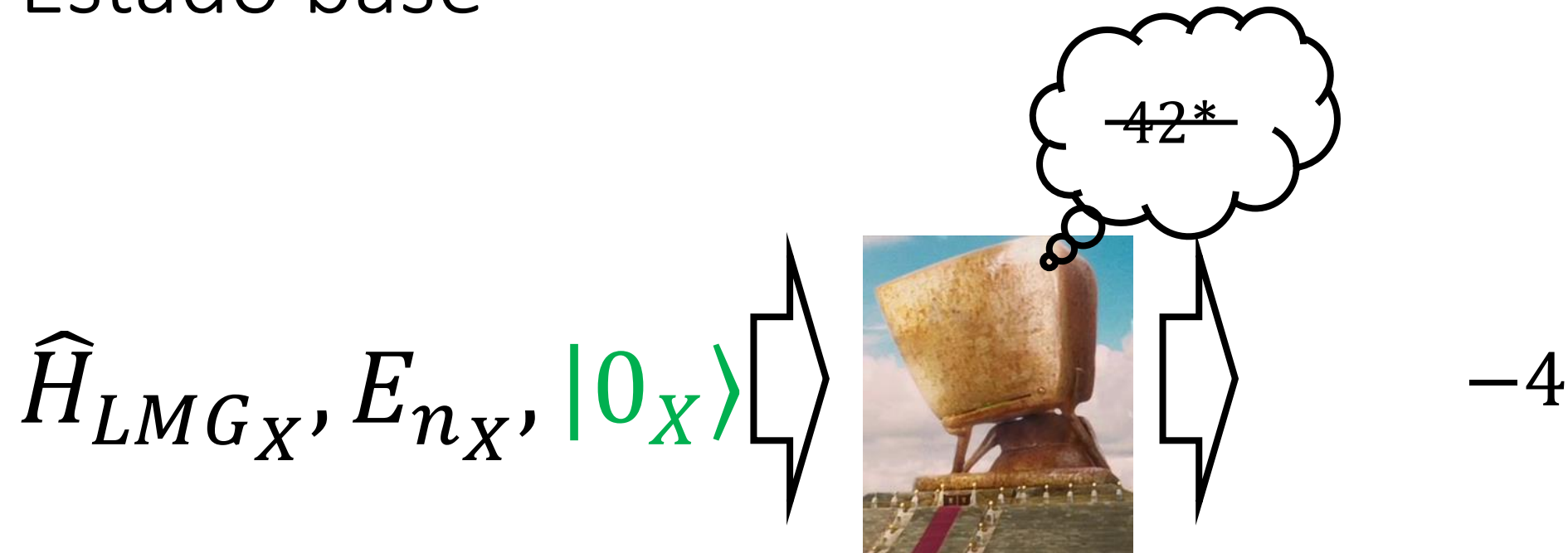
FIG. 6. Density of states when $\xi_y = 2$ and $\Omega_x = 0.2 \Omega_{xc}$ for $j = 256$. The red dashed line indicates the classical energy $e_1 = \sqrt{1 + \Omega_x^2} = 1.265$ where the ESQPT takes place.

Estado base

$$\hat{H}_{LMG_X}, E_{n_X}, |0_X\rangle \Rightarrow \text{Computer}$$

$$X = \{-6 < \Omega_x < 6\} \times \{0 < \xi_y < 3\}$$

Estado base



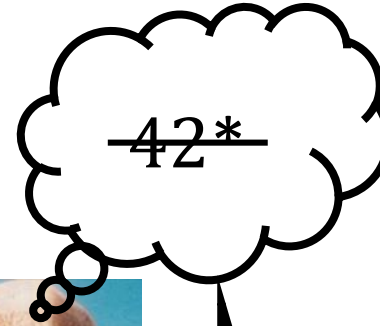
$$X = \{-6 < \Omega_x < 6\} \times \{0 < \xi_y < 3\}$$

*Movie: The Hitchhiker's Guide to the Galaxy (Guía del viajero intergaláctico)

Daniel Gutiérrez-Ruiz, Diego González, Jorge Chávez-Carlos, Jorge G. Hirsch and J. David Vergara, Physical Review B **103**, 174104 (2021)

Estado base

$$\hat{H}_{LMG_X}, E_{n_X}, |0_X\rangle$$



Resultado
Analítico

$$R = -4$$

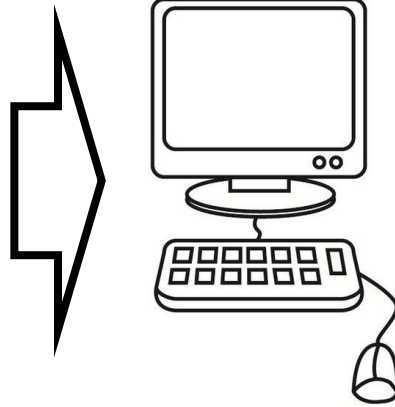
$$X = \{-6 < \Omega_x < 6\} \times \{0 < \xi_y < 3\}$$

*Movie: The Hitchhiker's Guide to the Galaxy (Guía del viajero intergaláctico)

Daniel Gutiérrez-Ruiz, Diego González, Jorge Chávez-Carlos, Jorge G. Hirsch and J. David Vergara, Physical Review B **103**, 174104 (2021)

Estado de máxima energía

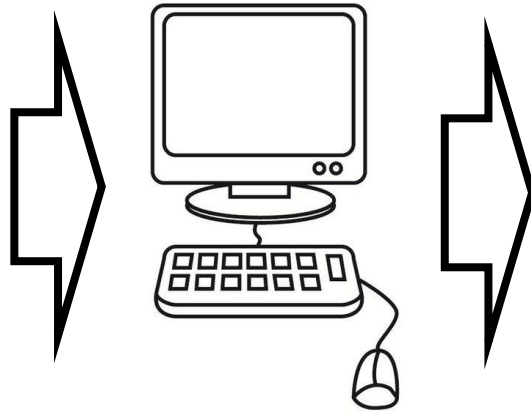
$$\hat{H}_{LMG_X}, E_{n_X},$$
$$|2j + 1_X\rangle$$



$$X = \{-6 < \Omega_x < 6\} \times \{0 < \xi_y < 3\}$$

Estado de máxima energía

$$\hat{H}_{LMG_X}, E_{n_X}, |2j + 1_X\rangle$$



$$X = \{-6 < \Omega_x < 6\} \times \{0 < \xi_y < 3\}$$

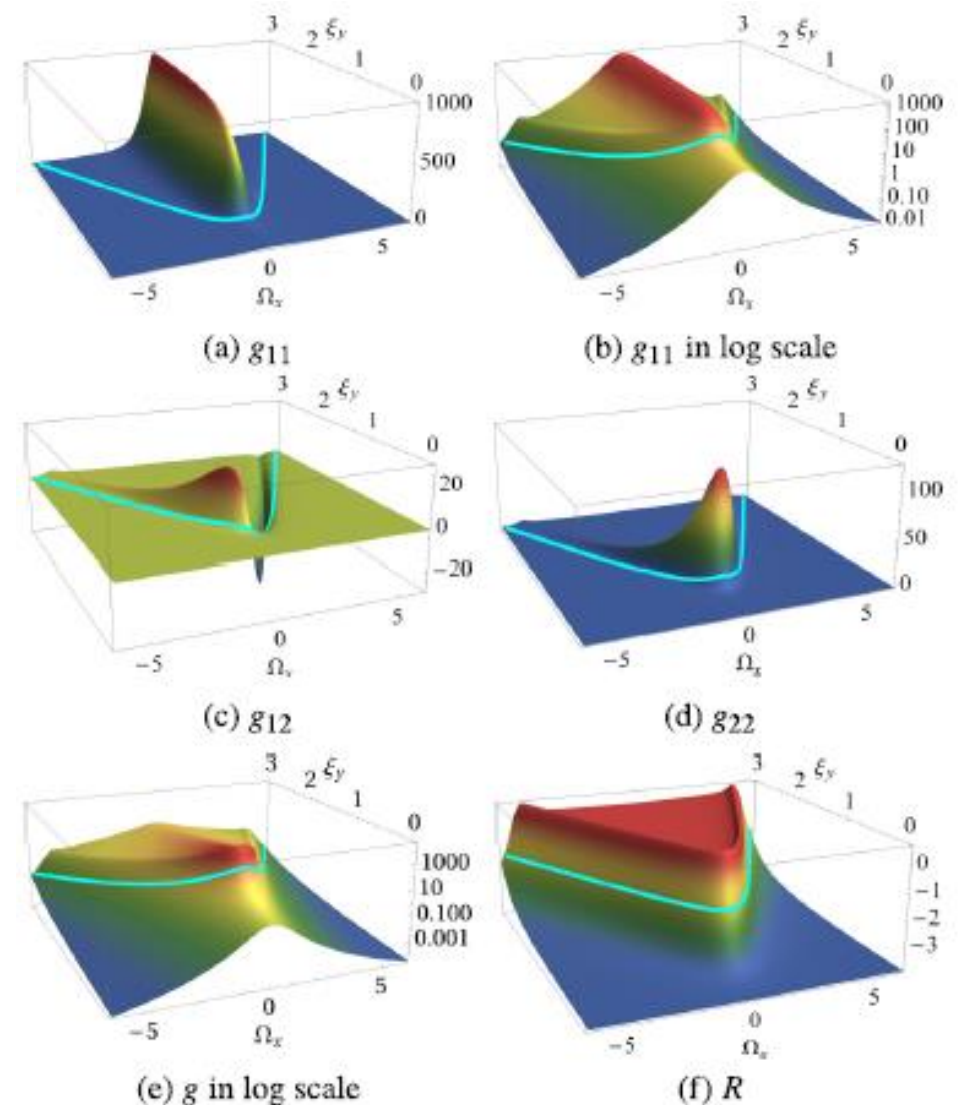
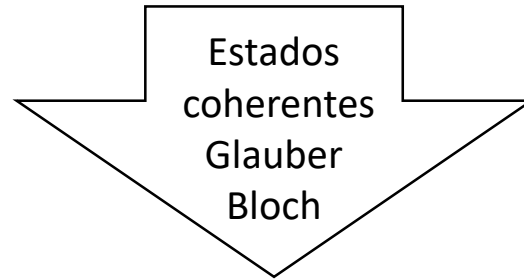


FIG. 10. QMT components and scalar curvature for the highest-energy state with $j = 32$. The cyan line is the separatrix given in Fig. 5(a) when $\xi_y = \frac{\sqrt{1+\Omega_x^2}}{2}$.

QMT en el modelo de DICKE

$$H_D = \omega a^\dagger a + \omega_0 J_z + \frac{\gamma}{\sqrt{\mathcal{N}}} (a + a^\dagger)(J_+ + J_-)$$



$$H_{cl} = \frac{\omega}{2}(p^2 + q^2) + \frac{\omega_0}{2}(P^2 + Q^2) + \gamma q Q \sqrt{4 - P^2 - Q^2} - \omega_0.$$

Con ω_0 fijo, espacio de parámetros $X = \{\gamma, \omega\}$

$$\gamma_c = \sqrt{\frac{\omega \omega_0}{2}}$$

Transición de Fase Cuántica (QPT)

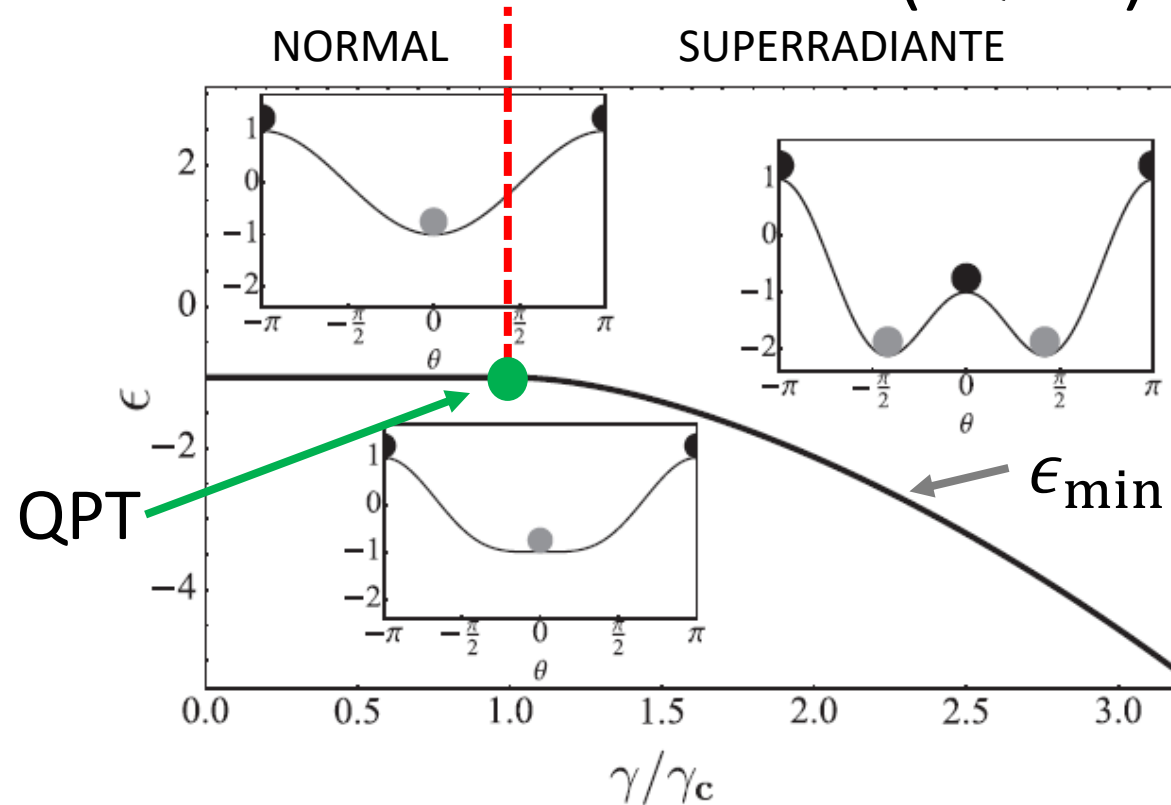


FIG. 2. Scaled energy minimum [$\epsilon_{\min} \equiv E_{\min}/(\omega_o j)$] as a function of the coupling constant measured with respect to the critical value (γ/γ_c).

$$\hat{H}_{D_X}, E_{n_X}^*, |n_X\rangle^*$$

M. A. Bastarrachea-Magnani, S. Lerma-Hernandez, and J. G. Hirsch, Phys. Rev. A **89**, 032101 (2014).

*M. A. Bastarrachea-Magnani and J. G. Hirsch, Phys. Scr. **T160**, 014005 (2014).

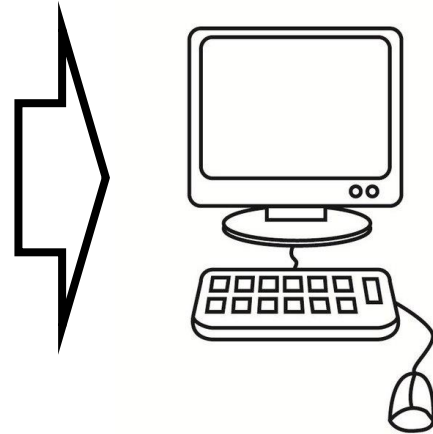
*J. G. Hirsch and M. A. Bastarrachea-Magnani, Phys. Scr. **T160**, 014018 (2014).

Estado base

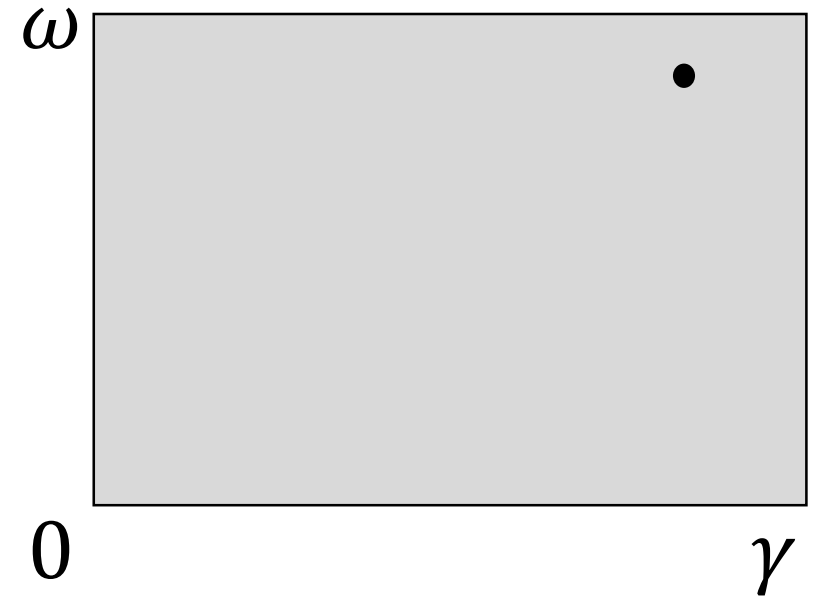
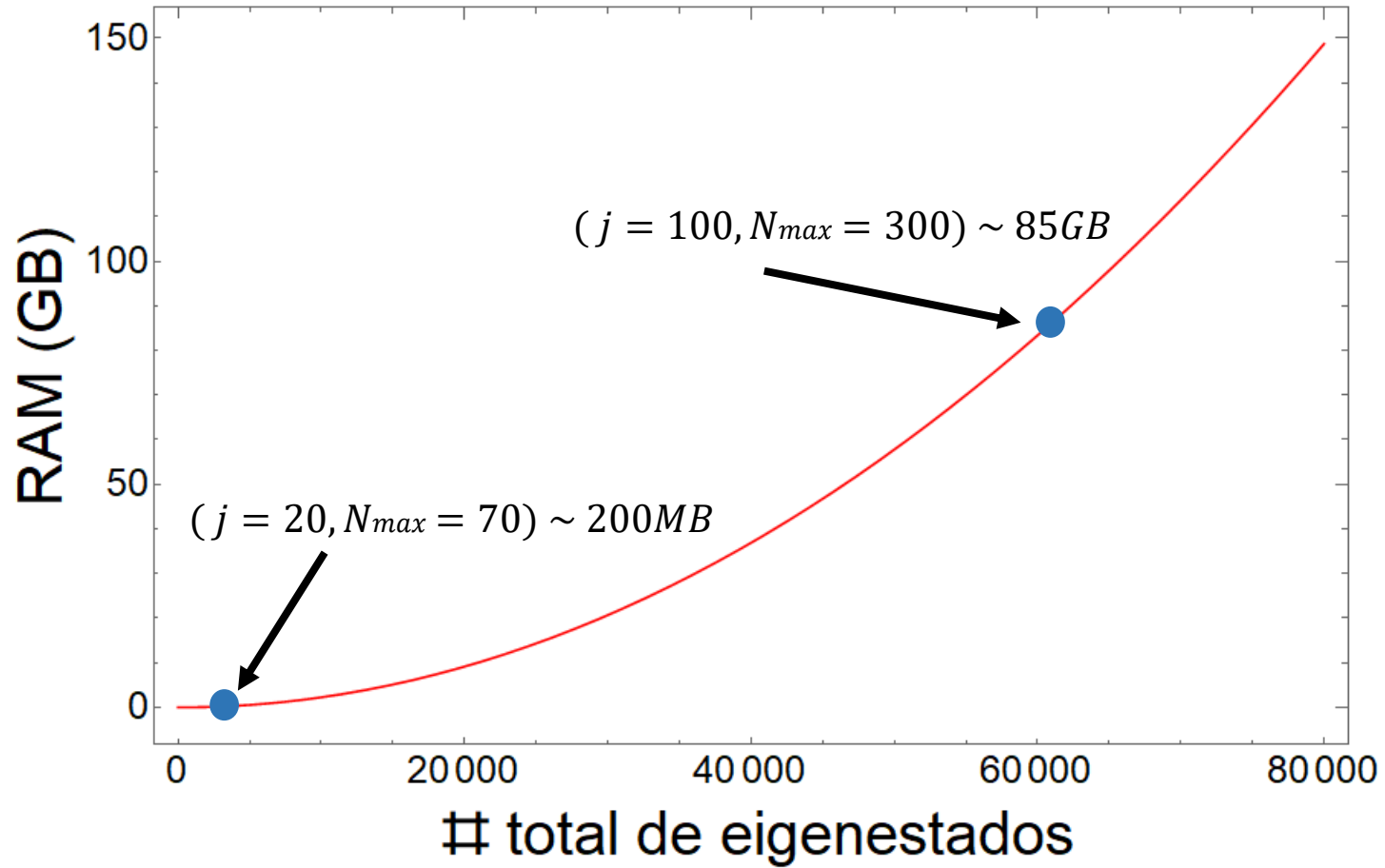
$$\hat{H}_{D_X}, E_{n_X}, |0_X\rangle$$

$$\omega_0 = 0.01, j = 20$$

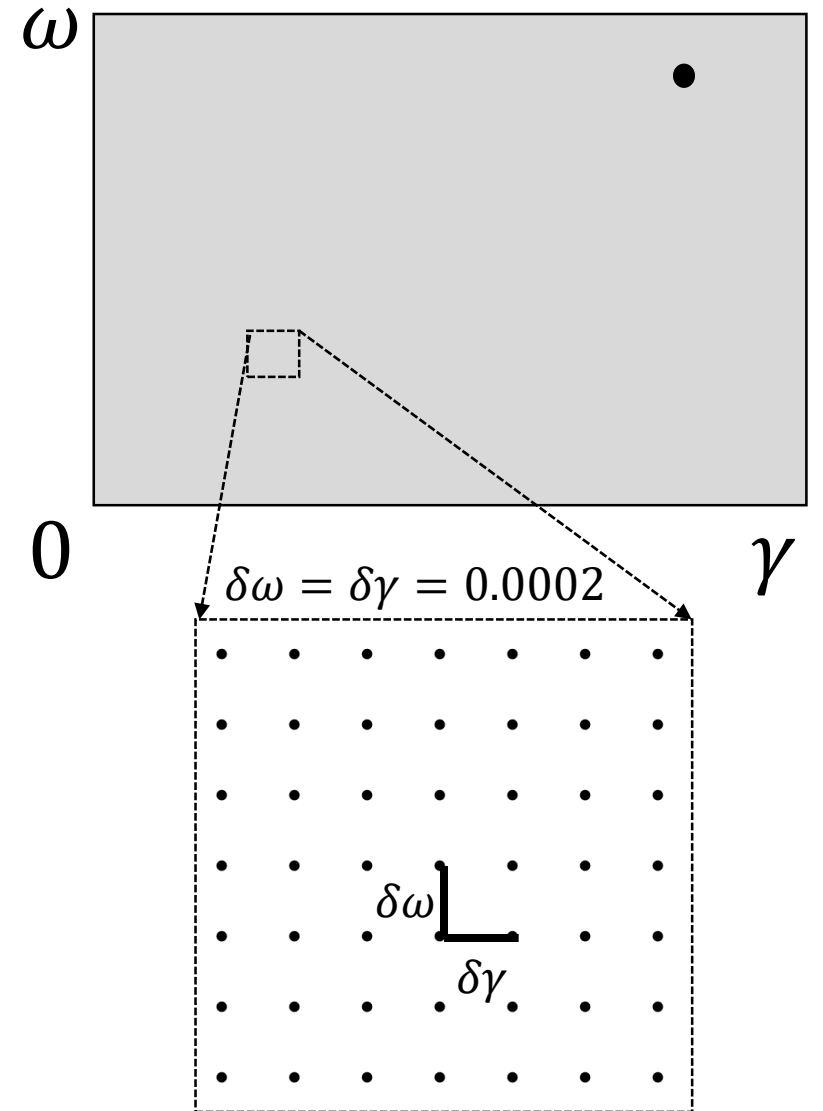
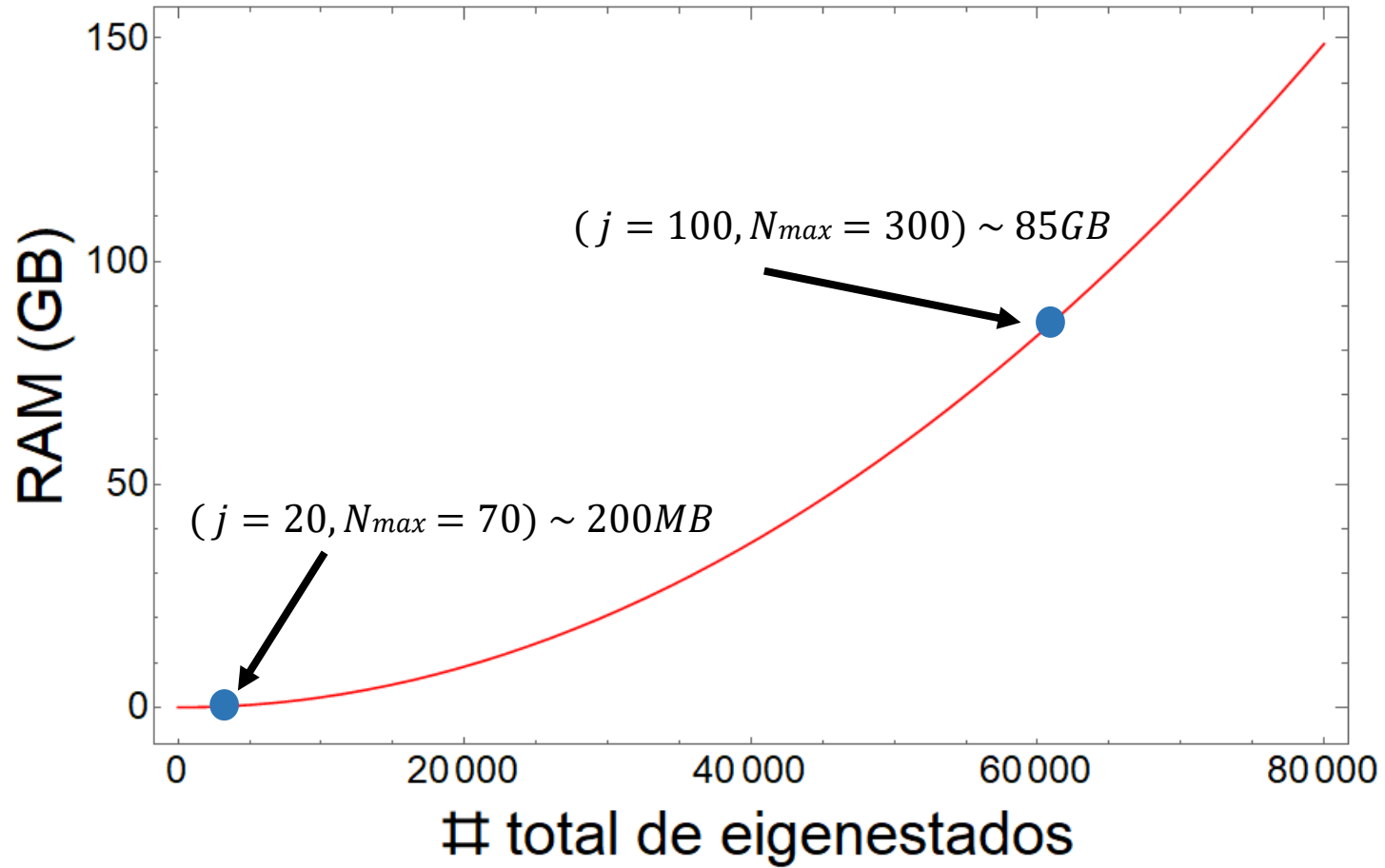
$$X = \{0.01 < \gamma < 0.05\} \times \{0.15 < \omega < 0.2\}$$



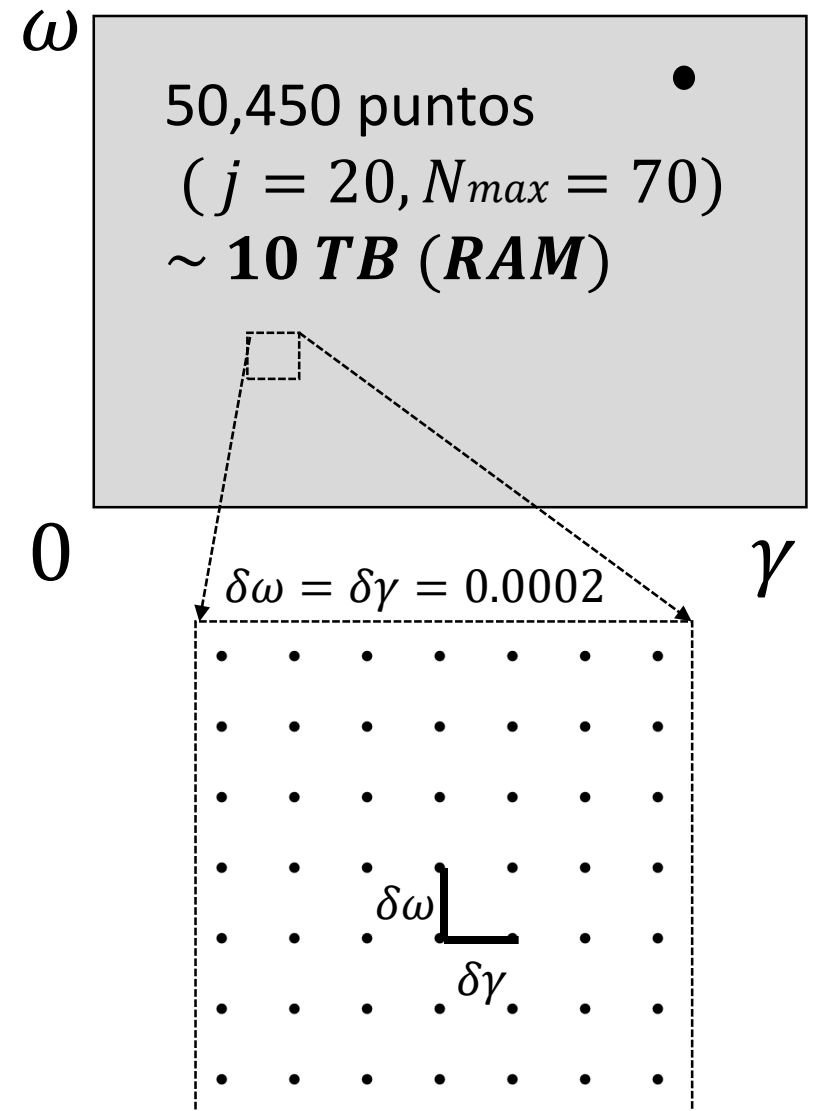
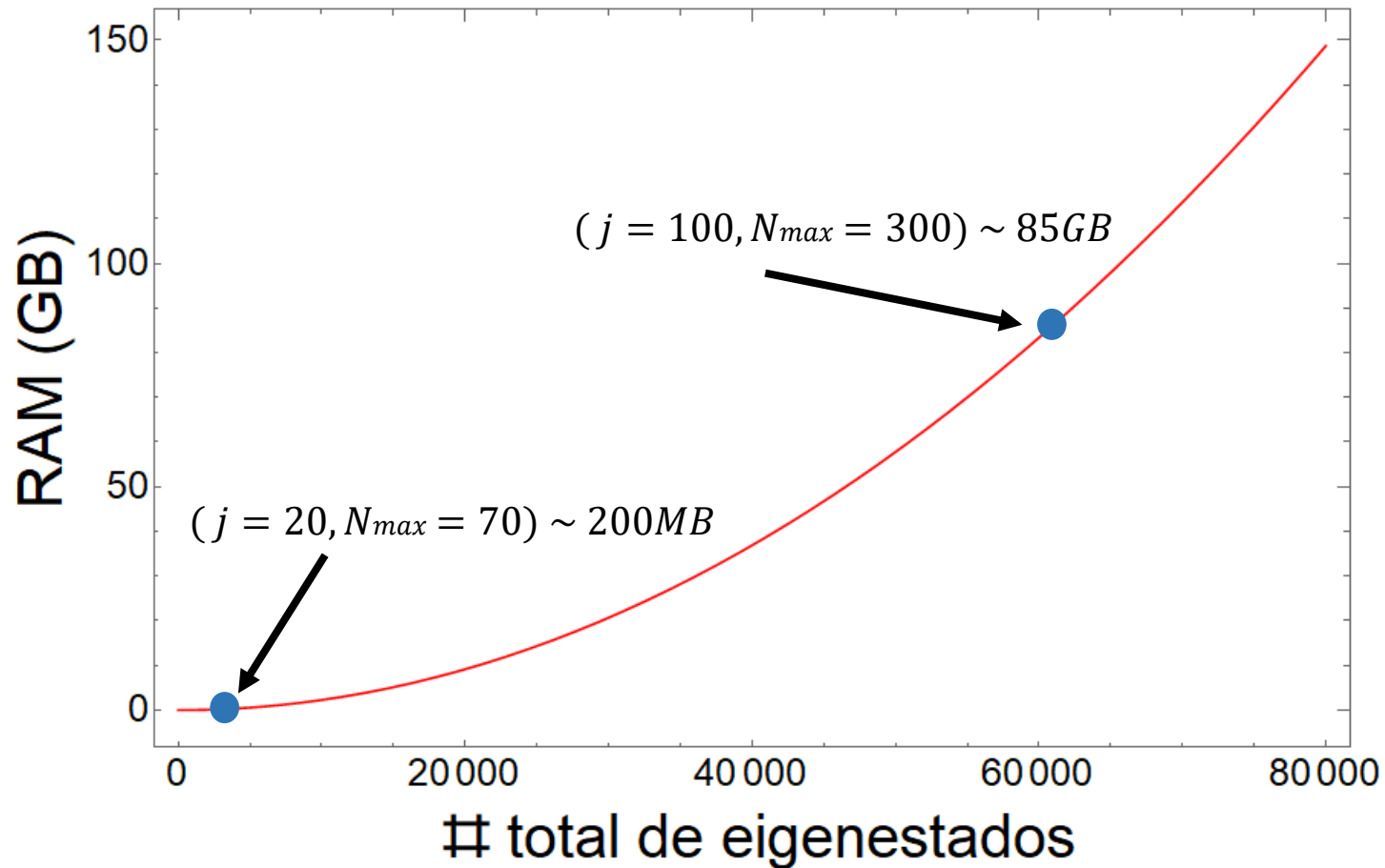
Recursos de cómputo



Recursos de cómputo



Recursos de cómputo



Estado base

$$\hat{H}_{D_X}, E_{n_X}, |0_X\rangle$$

$$\omega_0 = 0.01, j = 20$$

$$X = \{0.01 < \gamma < 0.05\} \times \{0.15 < \omega < 0.2\}$$

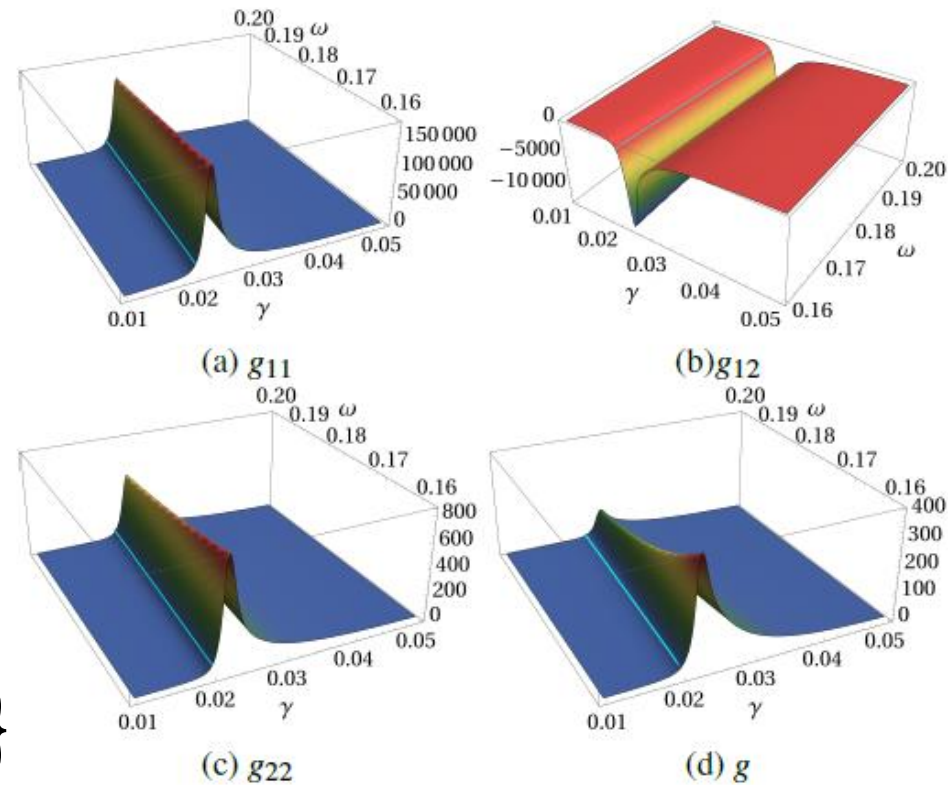
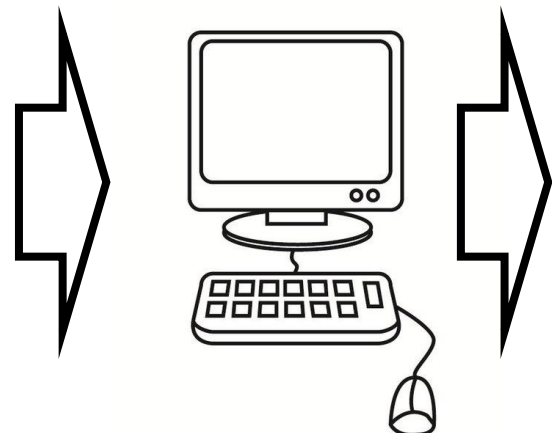


FIG. 6. QMT components in the case $j = 20$ with $\omega_0 = 0.01$. The cyan line is the separatrix.

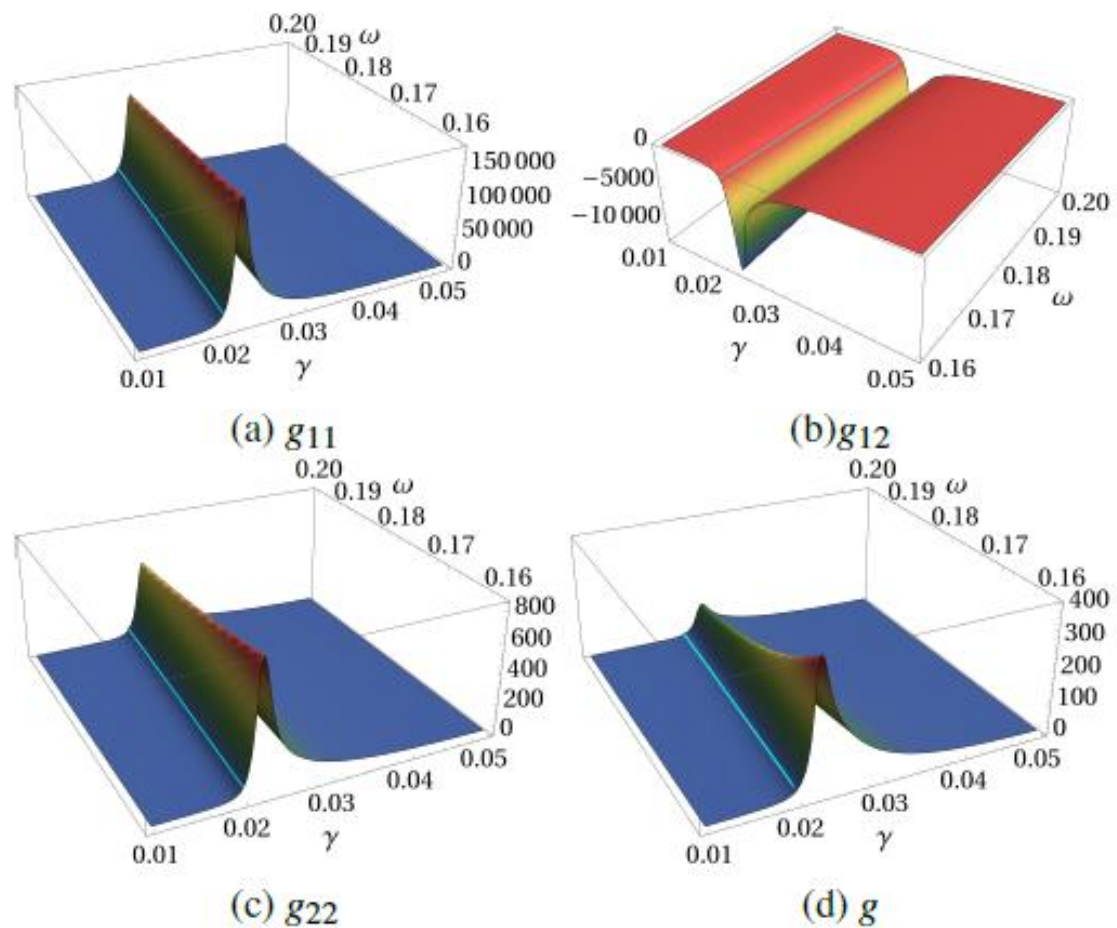


FIG. 6. QMT components in the case $j = 20$ with $\omega_0 = 0.01$. The cyan line is the separatrix.

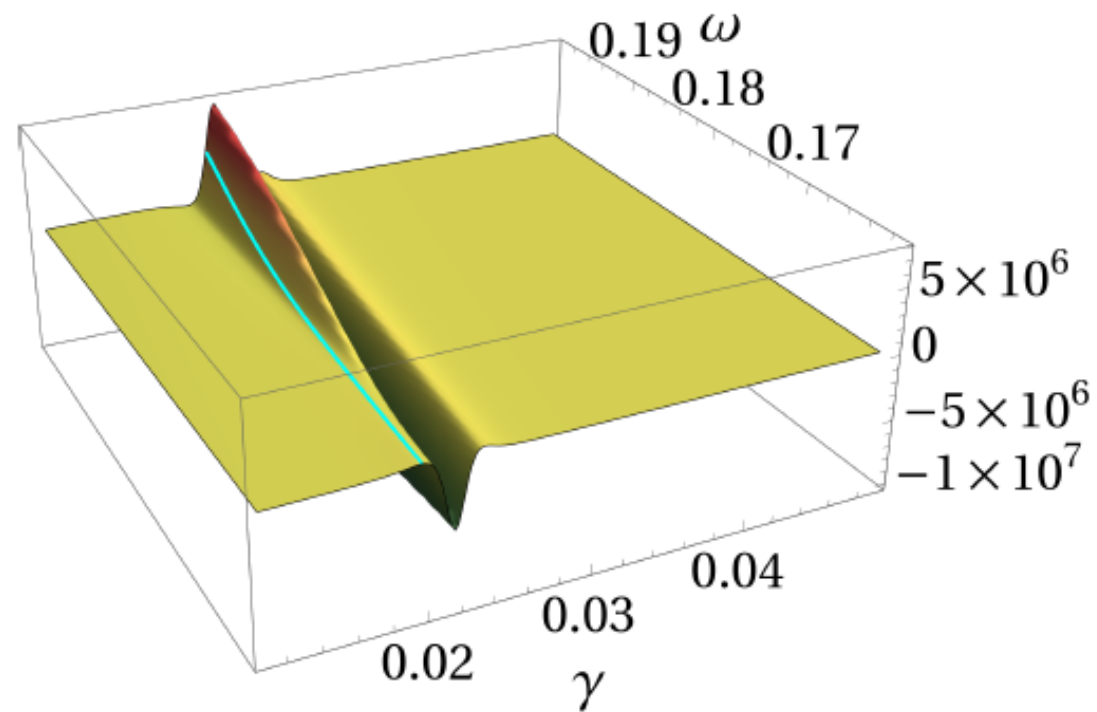


FIG. 7. Scalar curvature of the QMT in the case $j = 20$ with $\omega_0 = 0.01$. The cyan line is the separatrix.

Conclusiones

- Geometría cuántica ofrece alternativas enriquecedoras al estudio de las transiciones de fase cuánticas.
- Las componentes del QMT y el valor de R detectan la transiciones de fase en el modelo de LMG y en el modelo de Dicke.
- En el modelo de Dicke la detección de la transición de fase es observable con valores pequeños de j al emplear .
- Cálculos analíticos y numéricos para la obtención del QMT pueden ser operables ofreciendo soluciones indicativas de la existencia de transiciones de fase.
- Puede extenderse el análisis cantidades relevantes a la entropía por medio de la norma de Frobenius.

¡Gracias por su atención!



¡Gracias por su atención!